Long-term drought monitoring of the Zayandehrud River basin (central Iran) using hydroclimatological models and satellite observations

Babadi, Masoud; Iran Pour, Siavash; Roscher, Ribana; Amiri-Simkooei, Alireza; Karimi, Hamed

DOI
10.1117/1.JRS.16.014504

Publication date
2022

Document Version
Final published version

Published in
Journal of Applied Remote Sensing

Citation (APA)
Babadi, M., Iran Pour, S., Roscher, R., Amiri-Simkooei, A., & Karimi, H. (2022). Long-term drought monitoring of the Zayandehrud River basin (central Iran) using hydroclimatological models and satellite observations. *Journal of Applied Remote Sensing*, *16*(1), 1-27. Article 014504. https://doi.org/10.1117/1.JRS.16.014504

Long-term drought monitoring of the Zayandehrud River basin (central Iran) using hydroclimatological models and satellite observations

Masoud Babadi[a,*] **Siavash Iran Pour**[a,b] **Ribana Roscher**[c,d] **Alireza Amiri-Simkooei**[a,e] **and Hamed Karimi**[a]

[a]University of Isfahan, Department of Geomatics Engineering, Faculty of Civil Engineering and Transportation, Isfahan, Iran

[b]University of Isfahan, Research Institute of Environmental Studies, Isfahan, Iran

[c]Technical University of Munich, Department of Aerospace and Geodesy, Data Science in Earth Observation, Munich, Germany

[d]University of Bonn, Institute of Geodesy and Geoinformation, Remote Sensing, Bonn, Germany

[e]Delft University of Technology, Department of Geoscience and Remote Sensing, Delft, The Netherlands

Abstract. Drought is one of the most complex and threatening disasters, defined as a period of drier-than-normal conditions which results in water-related problems. In addition to climate variation, human activities can cause or intensify drought through groundwater overextraction, unsupervised expansion of agricultural lands, etc. One prime example of such drought has been observed in the Zayandehrud River basin in central Iran. We investigate the long-term (1986 to 2019) drought of the Zayandehrud River basin using meteorological, hydrological, and agricultural drought indices. The main focus of this research is to explore the impact of the irrigated area expansion in the upstream sub-basins on the agricultural drought of the downstream. To this end, different drought indices are employed over the whole basin and its sub-basins. The results indicate that the long-term precipitation index and snow reserves do not show a long-term trend during the study period, while the combined precipitation–evapotranspiration index and groundwater storage decline. The research concludes that the expansion of the agricultural lands in the river upstream, rising air temperature, and increasing population and industrial activities in the basin are most likely the driving forces to intensify the agricultural drought in the midstream and downstream parts of the basin. [DOI: 10.1117/1.JRS.16.014504]

Keywords: drought monitoring; Zayandehrud River; hydroclimatological models; satellite observations.

Paper 210509 received Aug. 9, 2021; accepted for publication Dec. 29, 2021; published online Jan. 13, 2022.

1 Introduction

Drought is considered as one of the most complex and threatening natural climate- and/or human-induced hazards; however, sufficient knowledge about this phenomenon has not been achieved yet.[1,2] Despite having no universal and unique definition, drought can be approximately defined as a shortage of water compared with normal conditions.[3,4] Droughts are classified into one of four types: meteorological drought (deficit of precipitation), hydrological drought (deficit of surface and groundwater storage), agricultural drought (deficit of root zone soil moisture or available water for plant growth), and socioeconomic drought (deficit of water for social or economic activities).[5,6] The first three drought types represent the natural and environmental effects, whereas the fourth one shows the impact on human population and society.[7,8] As already pointed

*Address all correspondence to Masoud Babadi, masoud.babadi92@gmail.com

1931-3195/2022/$28.00

out by Wilhite and Glantz,[5] these four types of drought are not independent, but they represent different methods for identification and measurement of drought.

Frequent drought events have significant impact on the hydrological cycle, ecological balance of ecosystems, vegetation cover, and agriculture. That is the case, in particular, with the recent severe drought events around the globe. As a result, the global attention to this issue has increased,[9,10] and therefore, numerous studies have been conducted in this field.[11–16] Because drought has a direct impact on agriculture and crop yields, especially in arid and semiarid regions, it is necessary to study this phenomenon in more detail. Although many recent drought events are caused by climate change, in many parts of the world human activities such as overextraction of groundwater and unsupervised expansion of agricultural lands have intensified the problem.[17–19] This kind of drought, mainly caused or intensified by human activities, is called "water bankruptcy" in the literature.[20] Prime examples of such droughts have been observed in arid and semiarid regions of the world, such as in the Middle East.[21–28] Two other examples are Refs. 29 and 30, which studied the human activities and the impact of meteorological condition on the Lake Urmia water level. In the latter work, the authors show the impact of the Urmia Lake Restoration Program, established in 2013, on the positive trend of the lake water level, water area, and water volume from 2015 to 2019, indicating a short-lived stabilization of Lake Urmia. In Ref. 31, the authors discuss the key gaps in our understanding of human influences on drought and potential feedbacks between drought and society where we need to acknowledge that human influence is as integral to drought as natural climate variability. The other work in Ref. 32 looks into drought definitions in which there is a need to revisit the definitions to explicitly include human processes as drivers. The research discusses that our understanding and analysis of drought need to move from single driver to multiple drivers and from unidirectional to multidirectional. The framework particularly provides a holistic view on drought in the Anthropocene, which can help us to improve management strategies for mitigating the severity and reducing the impacts of droughts in future. Reference 33 also presents an observation-based approach, the upstream–downstream comparison, to quantify changes in hydrological drought downstream of a human activity, as example in a basin in northern Chile. A sensitivity analysis of this research study is performed to assess how different choices of drought analysis threshold can affect the results and interpretation. In particular, the upstream–downstream comparison of the work includes the application of the upstream station threshold rather than the human-influenced downstream station.

In this study, we intend to accurately model long-term drought dynamics in the Zayandehrud River basin, located in central Iran, which has been significantly affected by drought over the two last decades. Tavazohi and Nadoushan[34] assessed the drought that occurred in the Zayandehrud River basin from 2000 to 2015 using the standardized precipitation index (SPI) and the normalized difference drought index (NDDI), as a combination of the normalized difference vegetation index (NDVI) and the normalized difference water index (NDWI). SPI assessment of their work implied that the condition in the basin was near normal or moderately dry, whereas NDDI showed an ascending trend during 2000 to 2015, i.e., significant drought condition. Safavi et al.[35] studied Zayandehrud River basin drought during 1983 to 2014. In their work, they made use of univariate drought indices including the standardized precipitation evapotranspiration index (SPEI), the standardized streamflow index, the standardized groundwater reservoir index, and the available water index as well as a multivariate drought index, namely, the hybrid drought index (HDI), which is based on states of climatic water balance and the available water. Moreover, they used a nonparametric approach presented by Farahmand and AghaKouchak,[36] in which univariate and multivariate drought indices have been calculated. The employment of the nonparametric approach was justified by coping with the challenges associated with parametric indices such as their sensitivity to the choice of parametric distribution functions. Through detecting drought onset, drought termination, and duration, their results concluded that their multivariate drought index HDI is preferable when compared with other univariate drought indices. Arast et al.[37] used the gravity recovery and climate experiment (GRACE) data and groundwater information from piezometric wells to estimate the monthly groundwater level changes in the Zayandehrud River basin during 2002 to 2018. The outputs of their work showed that underground water storage in the study time period is associated with the region rainfall; however, the water table storage does not respond to rainfall quickly. In fact, the

response has been incremental over the time period in which the drought events occurred in the river basin.

Abou Zaki et al.[38] investigated the impact of irrigation and drought on Zayandehrud River, groundwater, and the Gavkhuni Wetland (located at the end of the Zayandehrud River basin) using groundwater data from piezometric wells, GRACE data, and the drought indices including SPI, the streamflow drought index, and NDWI. Their results indicated that in more than half of the years of the period 1963 to 2012, the climate conditions are considered wet with respect to SPI while hydrological drought was recorded in most of the years in the Zayandehrud River flow. They also demonstrated the reconnection between surface water resources management and groundwater and showed that there is a direct relationship between the frequent occurrence of hydrological drought and human activities in the river basin.

According to the official reports, the area of irrigated agricultural fields in the Zayandehrud River basin has been doubled in the last 50 years which had led to environmental changes in the area.[39] Although some researches have been conducted on the drought of the basin, they have usually focused on the impacts of meteorological and hydrological parameters and the groundwater overextraction on the drought.[34,35,37,38] Those studies have mainly neglected the effect of irrigated area expansion in some sub-basins of the river basin on the drought occurred in the other parts of the basin.

Our research study tries to investigate the drought condition of the Zayandehrud River basin, in particular the impact of agricultural expansion in the upstream on the drought condition of the midstream and downstream of the basin. The research consists of the following sections: First, we introduce the study area and the datasets of our research work. Those datasets include reanalysis data and models, in addition to satellite observations. In the next section, we discuss the methodologies employed for extraction of drought indices from the datasets as well as methods for long-term trend analysis. The indices of this study are categorized in three groups: (i) meteorological drought indices including the SPI, the SPEI, and the standardized temperature index (STI), (ii) hydrological drought indices, including the snow water equivalent index (SWEI), the NDWI, and the GRACE drought severity index (GRACE-DSI), and (iii) an agricultural drought index, here, the vegetation condition index (VCI). The results section of this paper covers trend analysis of the aforementioned indices in the whole river basin as well as three selected sub-basins in the river basin. Those sub-basins are in the upstream, midstream, and downstream of the river basin, respectively. There, the trend behavior of the indices in each study region are cross-compared. In fact, the main focus of this study, presented in the results section, would be to investigate the effect of land cover changes, in particular through the irrigated area expansion, in the upstream sub-basins on the drought of the downstream sub-basins. Finally, we conclude our research through summarizing and discussing the results.

2 Study Area and Datasets

2.1 *Study Area*

The Zayandehrud River basin with an arid climate, located in central Iran, is selected as the study area of this research work. The basin covers an area of $41,524\ \text{km}^2$ and its elevation range varies from 1470 to 3974 m above the sea level; the annual precipitation of the basin varies in the range of 50 to 1500 mm where its annual average is about 130 mm.[38,40] The basin has been divided to 21 sub-basins by Isfahan Regional Water Board Organization (the authority for water allocation in the basin) (Fig. 1). The Zayandehrud River, as the largest river in central Iran, provides water for local irrigation, industries, municipal, supply, and animal farming.[41] The river has a length of 405 km, originating from Zagros mountains in the southwest of the country and ending in the Gavkhuni Wetland, although only a small amount of its water flow to the wetland.[42,43]

Due to many factors, such as the existence of deep and fertile soils and development of agricultural fields along Zayandehrud River, agriculture is the main water use in the basin. However, since the precipitation in the central and eastern parts of the basin is low, irrigation is very important for farming and uses 90% of the total consumed water even though only about 7% of the basin is covered by agricultural lands.[44,45] About 2600 km^2 of the basin is covered by agricultural irrigated fields which is mostly used for cultivating wheat, barely, silage plants,

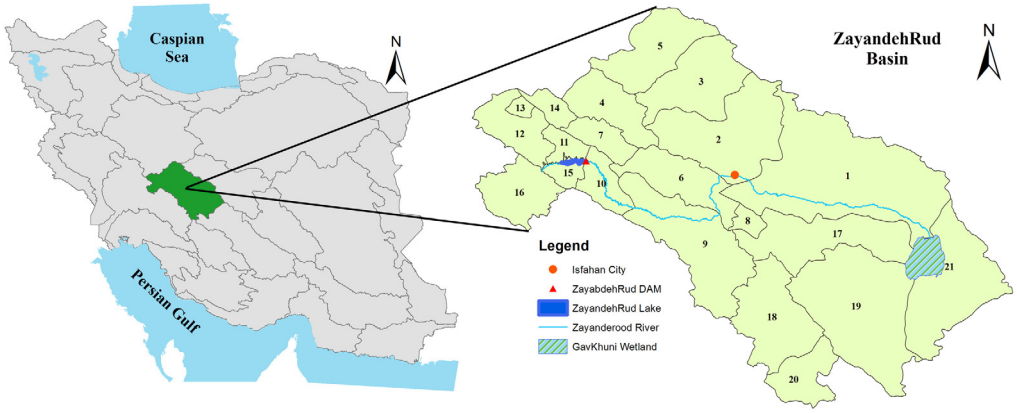

Fig. 1 Map of the Zayandehrud River basin as the study area. This map also shows the position of Zayandehrud River, Zayandehrud dam and lake, Isfahan City, and Gavkhuni Wetland.

potatoes, cotton, and paddy orchards.[43] The most important hydrological structure in the basin is Zayandehrud dam, which has a capacity of $15 \times 109\ m^3$and was built in 1972. Moreover, three main transbasin diversion tunnels have been constructed in 1952, 1985, and 2004, transferring about 660 Mm^3 water annually to the basin.[25,38,43] On the other hand, since 2002, outgoing transbasin water diversion projects for taking water from the Zayandehrud River to cities in the central desert of Iran such as Yazd, Kashan, etc., annually provide about 257 Mm^3 water to these regions.[25,43]

2.2 *Datasets*

2.2.1 *Precipitation (P)*

In this study, we make use of the monthly mean of total precipitation ERA5-Land dataset for evaluating meteorological drought. ERA5 is the atmospheric reanalysis dataset for the global climate produced by the European Centre for Medium-Range Weather Forecasts while ERA5-Land is a component of ERA5 which includes its land variables. Compared with the previous products, the ERA5-Land dataset contains a series of improvements such as higher spatial resolution and is more appropriate for land applications such as precipitation and evaporation. The dataset combines model data with observations from across the world into a globally complete and consistent dataset.[46,47]

2.2.2 *Potential evaporation*

Another ERA5 product used in our study is the monthly mean of the potential evaporation (PEV). PEV is produced by making a second call to the surface energy balance routine with the vegetation variables set to "crops/mixed farming" and assumes no stress from the soil moisture. Evaporation is computed for agricultural land as if it is well watered and through the assumption that the atmosphere is not influenced by this artificial surface condition.[46,48]

2.2.3 *Near-surface temperature*

The third ERA5 product used in the study is monthly mean of the air temperature at 2 m above the land surface. Considering atmospheric conditions, the dataset is produced by interpolation between the lowest model level and the Earth's surface.[46]

2.2.4 *Snow water equivalent*

In this study, we employ the snow water equivalent (SWE) dataset of the FLDAS (FEWS NET land data assimilation system). FLDAS dataset contains many climate-related information, such

as humidity, evapotranspiration, moisture content, and average soil temperature. Those products aim to help with food security assessments in data-sparse, developing country settings.[49] FLDAS is a custom instance of the National Aeronautics and Space Administration (NASA) Land Information System (LIS).[50] Among multiple FLDAS datasets that use different land surface models, here, we use FLDAS with Noah version 3.6.1 surface model. The dataset is driven by the Climate Hazards Group InfraRed Precipitation with Station (CHIRPS) rainfall dataset and the NASA's Modern-Era Retrospective analysis for Research and Applications version 2 (MERRA-2) meteorological forcing,[49] where CHIRPS is a quasiglobal rainfall dataset designed for seasonal drought monitoring and trend analysis.[51]

2.2.5 *Water area*

To monitor the Gavkhuni Wetland and Zayandehrud Lake water area fluctuations, monthly Landsat surface reflectance images are employed. For our study period (1986 to 2019), Landsat 5 (for the period of 1986 to 1999), Landsat 7 (for the period of 1999 to 2013), and Landsat 8 (for the period of 2013 to 2019) images are utilized. The repeat cycle of all three Landsat satellites is 16-day, and if more than one image was available in each month, the mean was used for water area calculation. Based on trial and error, specifically for our study region, the cloud cover of all our images is chosen to be <20%, which means selected images are cloud-free or nearly cloud-free.

2.2.6 *Total water storage anomaly*

In this study, total water storage (TWS) dataset of the GRACE and GRACE-FO satellite missions is used in the period of 2002 to 2019. The GRACE mission was launched in March 2002 and ended in June 2017. The GRACE mission provided surface mass change from observing Earth's time-dependent gravity field. The monthly terrestrial water storage (TWS) anomalies, a very important variable for land hydrological applications, is derived from the surface mass change after removing the atmospheric and oceanic contributions.[52,53] TWS demonstrates monthly fluctuation of the TWS in the terrestrial environment including surface water, soil moisture, ground water, and snow.[38] Since June 2018, the GRACE Follow-On (GRACE-FO) is extending the 15-year monthly mass change record of the GRACE mission.

2.2.7 *Groundwater level fluctuation*

For evaluating the groundwater level fluctuation in the basin, we use groundwater depletion rate for each aquifer. This data are provided by Isfahan Regional Water Board Organization.

2.2.8 *Vegetation coverage and status*

To monitor the long-term (1986 to 2019) surface vegetation coverage and activities, here, we employ NOAA CDR of AVHRR NDVI. The dataset contains gridded daily NDVI derived from the NOAA AVHRR surface reflectance product, provided in a spatial resolution of 0.05 deg and computed globally over the land surface. NOAA CDR of AVHRR NDVI is produced using eight NOAA satellites including NOAA-7, -9, -11, -14, -16, -17, -18, and -19, available from 1981 to the present time. In this work, we use Version 5 of the dataset, which contains a series of improvements including use of the improved surface reflectance and the corrections for the known errors in time, latitude, and longitude variables. This dataset is a part of Land Surface CDR Version 5 products generated by the University of Maryland (UMD) and the NASA Goddard Space Flight Center (GSFC).[54]

3 Methodology

In this section, we present the framework of the study for investigating the basin long-term drought. Comparing with the raw data, the drought indices are more readily useable and provide

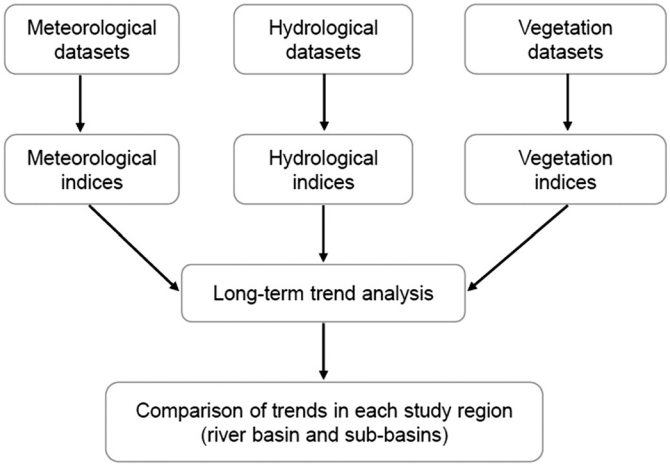

Fig. 2 The workflow of long-term drought monitoring in the Zayandehrud River basin.

complete insight for decision making and drought analysis.[55] In this study, we use standardized anomaly index,[56] conditional drought indices,[57,58] and nonparametric standardized drought indices[36] for drought monitoring. Those indices are presented in the following sections. Figure 2 and Table 1 summarize the workflow and dataset of this study, respectively. It is important to mention that different datasets of this research work own different temporal and spatial resolutions. However, for the purpose of our work, all datasets are averaged over months and river basin and sub-basins. The only exception is the water surface and therefore its corresponding index NDWI, which are monthly averaged over three selected areas along the river. We also utilize the data sources over a long time span, thus providing meaningful drought analysis.

3.1 *Standardized Anomaly Index*

For monitoring hydrological drought using GRACE data, a standardized anomaly index namely GRACE-DSI is used.[56,59] GRACE-DSI for each grid cell is defined as the standardized anomalies of GRACE TWS as follows:

$$\text{GRACE-DSI}_{i,j} = \frac{\text{TWS}_{ij} - \overline{\text{TWS}_J}}{\sigma_j}, \tag{1}$$

where i is the year, j is the month, and $\overline{\text{TWS}_J}$ and σ_j are the mean and standard deviation of TWS anomalies in month j, respectively. This index is dimensionless and detects both drought and

Table 1 Summary of datasets and the extracted indices used in the study.

Parameters	Indices	Dataset
Meteorological parameters	SPI	ERA-5-Land monthly mean of precipitation
	SPEI	ERA-5 monthly mean of precipitation and PEV
	STI	ERA-5 monthly mean of near-surface temperature
Hydrological parameters	SWEI	FLDAS SWE monthly mean
	NDWI	Green and NIR bands of the Landsat images (monthly mean)
	GRACE-DSI	GRACE and GRACE-FO TWS monthly solutions
Vegetation parameter	NDVI	Red and near-infrared of the spectral reflectance measurements from NOAA CDR of AVHRR (monthly mean)
	VCI	Based on monthly-mean NDVI and its long-term minimum and maximum from NOAA CDR of AVHRR

Table 2 Drought classification based on GRACE-DSI values.

Drought categories (description)	GRACE-DSI values
D5 (exceptional drought)	GRACE-DSI ≤ -2
D4 (extreme drought)	$-1.99 \leq$ GRACE-DSI ≤ -1.6
D3 (severe drought)	$-1.59 \leq$ GRACE-DSI ≤ -1.3
D2 (moderate drought)	$-1.29 \leq$ GRACE-DSI ≤ -0.8
D1 (abnormally dry)	$-0.79 \leq$ GRACE-DSI ≤ -0.5
N (Near normal)	$-0.49 \leq$ GRACE-DSI ≤ 0.49
W1 (slightly wet)	$0.5 \leq$ GRACE-DSI ≤ 0.79
W2 (moderately wet)	$0.8 \leq$ GRACE-DSI ≤ 1.29
W3 (very wet)	$1.3 \leq$ GRACE-DSI ≤ 1.59
W4 (extremely wet)	$1.6 \leq$ GRACE-DSI ≤ 1.99
W5 (exceptionally wet)	$2 \leq$ GRACE-DSI

abnormally wet events. The GRACE-DSI can be classified into drought categories based on the thresholds of cumulative relative frequency for GRACE-DSI values[56] (Table 2).

3.2 *Condition Drought Indices*

In this study, a condition index namely VCI is used for drought monitoring which is based on NDVI. VCI is a prevalent drought index that is employed for agricultural drought monitoring,[2,60–65] related to the long-term minimum and maximum NDVI.[57] The index scales pixel NDVI value between its maximum and minimum values for a given period and can be expressed as

$$\mathrm{VCI}_{ijk} = \frac{\mathrm{NDVI}_{ijk} - \mathrm{NDVI}_{jk,\min}}{\mathrm{NDVI}_{jk,\max} - \mathrm{NDVI}_{jk,\min}}, \tag{2}$$

where NDVI_{ijk} is the monthly NDVI for pixel k in month j ($j = 1, 2, \ldots, 12$) for year i, and $\mathrm{NDVI}_{jk,\min}$ and $\mathrm{NDVI}_{jk,\max}$ denote the multiyear minimum and maximum NDVI, respectively, for pixel k in month j. The variation range of VCI is from 0 to 1, corresponding to change in vegetation condition from extremely bad to optimal.[58,66] Drought severity for the condition drought indices is classified into six categories based on the literature[2,63] (Table 3).

Table 3 Drought classification based on VCI values.

Drought classes	VCI values
Extreme drought	$0 \leq$ VCI < 0.1
Severe drought	$0.1 \leq$ VCI < 0.2
Moderate drought	$0.2 \leq$ VCI < 3
Mild drought	$0.3 \leq$ VCI < 0.4
Abnormally dry	$0.4 \leq$ VCI < 0.5
No drought	$0.5 \leq$ VCI ≤ 1

3.3 *Nonparametric Standardized Drought Indices*

Different indicators have various ranges and scales, so in most cases, it is not possible to compare their values directly. One of the attractive features of standardized indices is that they are statistically consistent. For having a comprehensive drought monitoring, it is important to investigate multiple indicators, such as precipitation and runoff, which often have different distribution functions.[35,36] Several parametric standardized indices (such as SPI which frequently uses the two-parameter gamma distribution function) are sensitive to the choice of parametric distribution functions.[67,68] To cope with these challenges, we use a nonparametric methodology to handle different hydrological variables that does not rely on representative parametric distribution. Farahmand and AghaKouchak (2015) introduced the standardized drought analysis toolbox offering a nonparametric framework for deriving univariate and multivariate standardized indices.[36]

To derive a nonparametric standardized index (SI), the empirical Gringorten plotting position, suggested by Hao and AghaKouchak,[69] is employed in our study. The formulation follows as[70]

$$p(x_i) = \frac{r - 0.44}{n + 0.12}, \tag{3}$$

where n is the sample size, r denotes the rank of the observed values in descending order, and $p(x_i)$ is the corresponding empirical probability of variable x which is each one of the observation sets (e.g., precipitation) at a specific time scale such as 1, 3, or 6 months. The outputs can be transformed into SI as follows:

$$SI = \phi^{-1}(p), \tag{4}$$

where p is the probability derived from Eq. (3) and ϕ is the standard normal distribution function.

In this research work, SPI, SPEI, STI, and SWEI are calculated using the nonparametric SI. The calculation of SPI, SPEI, STI, and SWEI is based on P, difference between P and PEV (P-PEV),[71] near-surface temperature, and SWE datasets. The nonparametric standardized drought indices, similar to the parametric indices, can be presented by D-scale drought categories as tabulated in Table 4.[36,72]

3.4 *Normalized Difference Water Index*

For monitoring water area change in our study, we make use of NDWI,[73] as a frequently used information for water body estimation.[74–76] The formulation follows as

$$\mathrm{NDWI} = \frac{x_{\mathrm{Green}} - x_{\mathrm{NIR}}}{x_{\mathrm{Green}} + x_{\mathrm{NIR}}}, \tag{5}$$

where x_{Green} and x_{NIR} refer to pixel values in the green and NIR bands of Landsat satellites, respectively. x_{Green} and x_{NIR} are corresponding to band 2 and band 4 in Landsat 5 and 7 and band 3 and band 5 in Landsat 8, respectively.

Table 4 Drought classification based on nonparametric standardized drought indices.

Drought categories (description)	SI values
D4 (exceptional drought)	$SI \leq -2$
D3 (extreme drought)	$-1.99 \leq SI \leq -1.6$
D2 (severe drought)	$-1.59 \leq SI \leq -1.3$
D1 (moderate drought)	$-1.29 \leq SI \leq -0.8$
D0 (abnormally dry)	$-0.79 \leq SI \leq -0.5$

3.5 *Time-Series Trend Analysis*

Time-series in the study are analyzed using the classical Student's t-test[77] and Mann–Kendall (MK) nonparametric test,[78,79] where the purpose is to evaluate the presence of a trend in time series.

3.5.1 *Student's t-test*

A t-test is used as a hypothesis testing tool and is applied commonly when the test statistic follows a normal distribution. The t-test statistic is actually the ratio of the estimate of the trend's slope to its standard deviation. In this way, the test assesses the presence of trend by its magnitude.[80]

3.5.2 *Mann–Kendall nonparametric test*

This test has been widely used to analyze trends in different climate variables.[19,81,82] The MK test statistics is defined as

$$S_{\mathrm{MK}} = \sum_{i=1}^{N} \sum_{j=i+1}^{N} \mathrm{sgn}(x_j - x_i), \quad \mathrm{sgn}(x_j - x_i) = \begin{cases} +1 & x_j > x_i \\ 0 & x_j = x_i \\ -1 & x_j < x_i \end{cases}, \tag{6}$$

where n is the length of the time-series and x_i and x_j are the data values in the time-series. In the test, each data point is successively treated as a reference point and is compared with all data points that follow in time.[19,83] Once N is greater than 8, S_{MK} values follow an approximately normal distribution[84] which its variance is defined as

$$\sigma^2_{S_{\mathrm{MK}}} = \frac{N(N-1)(2N+5)}{18}. \tag{7}$$

Finally, the MK test statistics Z_{MK} is given as

$$Z_{\mathrm{MK}} = \begin{cases} \frac{S_{\mathrm{MK}}-1}{\sigma_{S_{\mathrm{MK}}}}, & S_{\mathrm{MK}} > 0 \\ 0, & S_{\mathrm{MK}} = 0 \\ \frac{S_{\mathrm{MK}}+1}{\sigma_{S_{\mathrm{MK}}}}, & S_{\mathrm{MK}} < 0 \end{cases}. \tag{8}$$

A positive Z_{MK} value indicates a positive trend in the time-series and vice versa. The Z_{MK} is also used to test the null hypothesis H_0 which means "there is no significant trend." When $|Z_{\mathrm{MK}}| > 1.96$, H_0 is rejected at 5% significance level (p-value < 0.05).

4 Results

In this section, we survey the long-term trend of the proposed drought indices. The section consists of two parts. First, we look into the whole river basin where the long-term trend of meteorological, hydrological, and agricultural drought indices are analyzed. In the second part, the analyses are performed in the sub-basins, where the focus is to investigate the effect of land cover changes in the river upstream area on the drought of the downstream part. There, we take a closer look into a few different sub-basins on upstream (sub-basin 10), midstream (sub-basin 6), and downstream (sub-basin 1), as examples.

In addition to monthly time-series analysis, we study the time-series of the month "May," since this month of year has particular importance in agricultural activities in the region. To investigate the impact of time scales on the vegetation response, different scenarios are utilized in this research work. We analyze the trend line slopes and the significance of trends through the results of t-test and MK test. However, since different indices have different ranges, the trend line slopes throughout the paper are calculated based on normalized data between 0 and 1. The normalization then makes the trend slopes comparable. We specifically visualize 3-month and 9-month timespans, since they can be considered as good representative for short-term and almost long-term accumulations in climate studies.

4.1 *Drought Analysis of the Zayandehrud River Basin*

4.1.1 *Meteorological drought*

To study the meteorological drought in the basin, SPI, SPEI, and STI information are employed. For SPI and SPEI, we use different timespans of SPI (SPI-1, SPI-3, etc.) and SPEI (SPEI-1, SPEI-3, etc.) for two scenarios of "all months" and "months May." Similarly, STI in the case of "all months" and "months May" and for different timespans are also used for assessing the changes in near-surface air temperature. A few examples of the aforementioned times-series along with their trends and the associated trend line slope (m), MK-test, and t-test results are shown in Fig. 3.

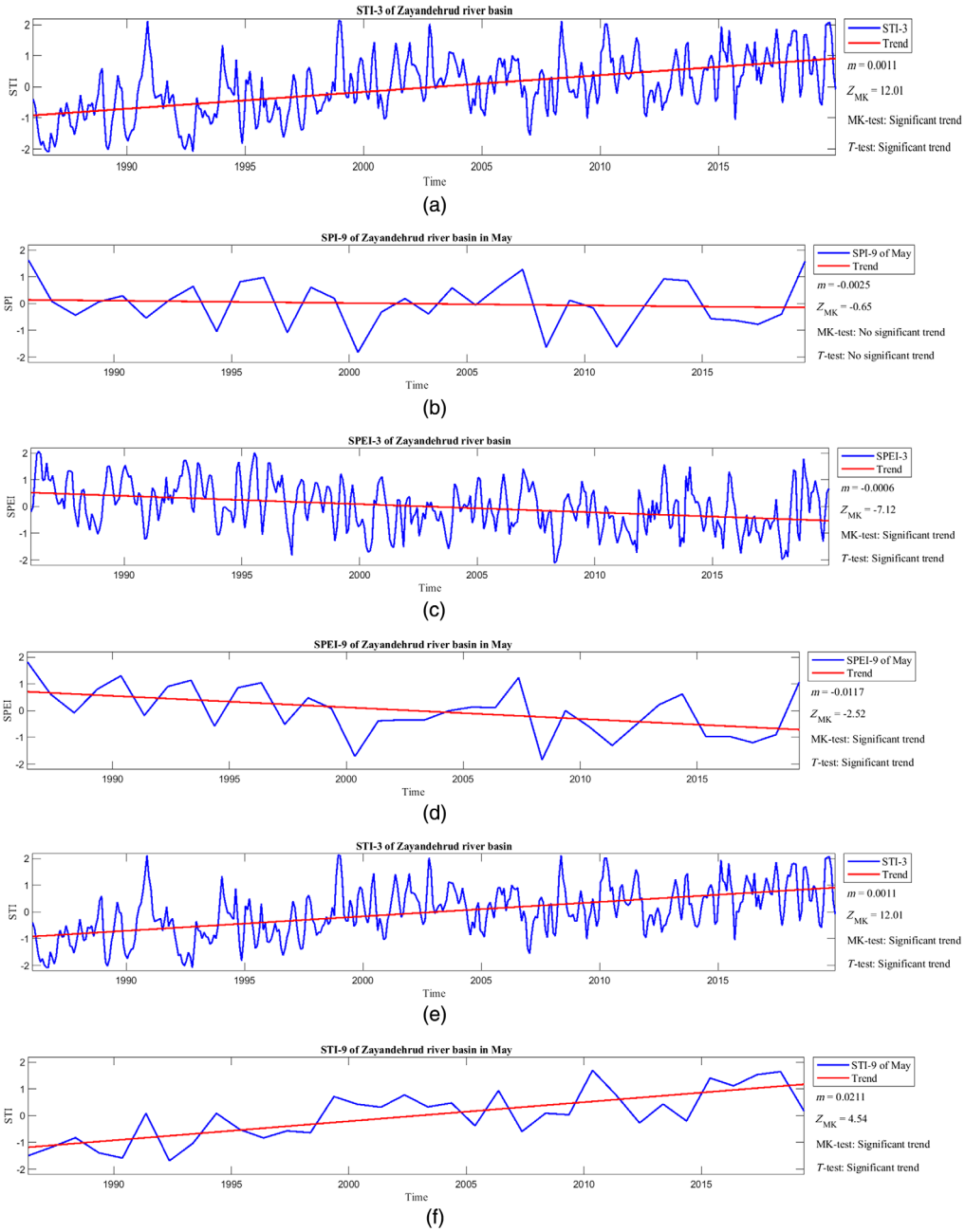

Fig. 3 (a) SPI-3 "all months," (b) SPI-9 in "months May," (c) SPEI-3 "all months," (d) SPEI-9 in "months May," (e) STI-3 "all months," and (f) STI-9 in "months May" calculated in the basin.

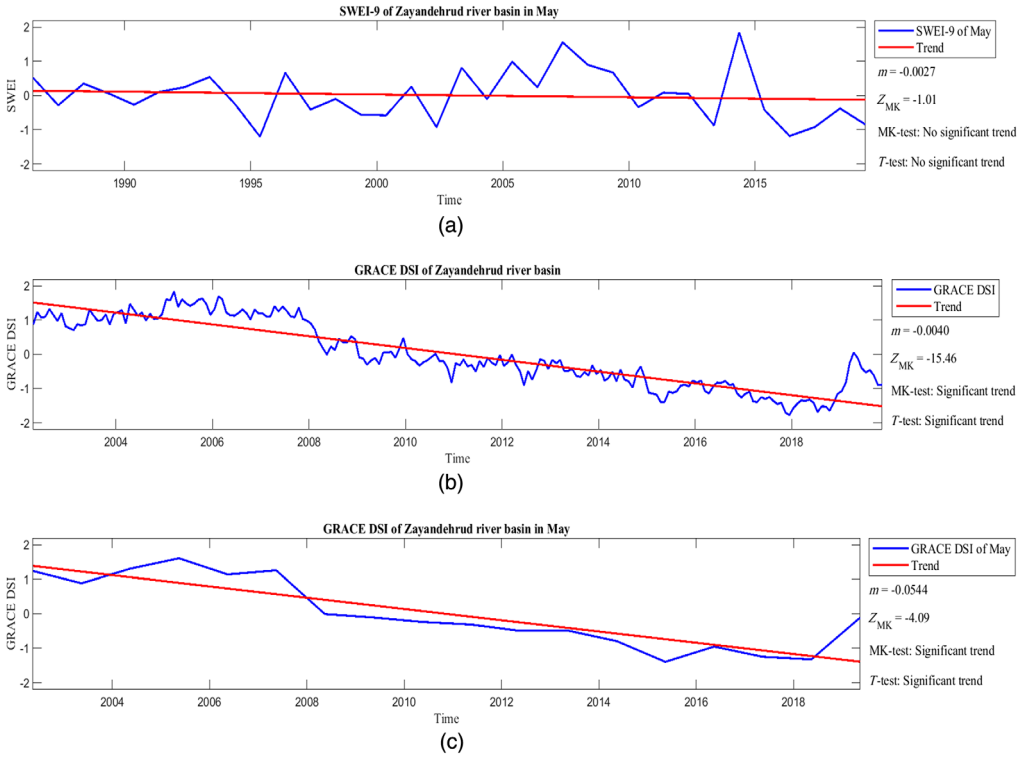

Fig. 4 (a) SWEI-9 in "months May," (b) GRACE-DSI, and (c) GRACE-DSI in "months May," calculated in the basin.

As it can be seen from the results, no trend is detected in monthly SPI-3 and SPI-9 in "months May," which indicates the precipitation has no overall descending or ascending trend in the basin in the whole study period for those timespans. However, in the case of SPEI, we observe descending trend for both SPEI-3 "all months" ($Z_{MK} = -7.12$) and SPEI-9 in "months May" (-2.52). On the other hand, the results of STI show that both STI-3 "all months" and STI-9 in "months May" have significant ascending trends, implying that the near-surface air temperature has increased during the given period.

4.1.2 *Hydrological drought*

Assessing the hydrological drought, SWEI and GRACE-DSI indices in the basin are utilized. Here, we evaluate SWE through SWEI for different timespans for "months May." To monitor the water level depletion, monthly GRACE-DSI and GRACE-DSI in "months May" are employed. Examples of the results are shown in Fig. 4.

Based on the results of the examples in Fig. 4, the trend of SWEI-9 in "months May" is not recognized as significant. On the contrary, both monthly GRACE-DSI and GRACE-DSI in "months May" show significant descending trends.

4.1.3 *Agricultural drought*

Agricultural drought is the response of the vegetation condition to meteorological and hydrological drought. For monitoring the vegetation condition in the basin, vegetated area change in "months May" as agricultural growth period, the monthly VCI, and VCI in "months May" of the basin are estimated and employed for our analysis. Based on several experiments, a threshold of 0.2 is applied on NDVI values for the vegetated area change, where pixels greater than the threshold are considered as vegetated pixels. The monthly vegetated area change and VCI time series are shown in Fig. 5. As it is clear from the figure, the trend of vegetated area change in the period of 1986 to 2019 is not recognized as significant, while both monthly VCI and VCI in "months May" show significant descending trends in the basin. As an example, VCI change

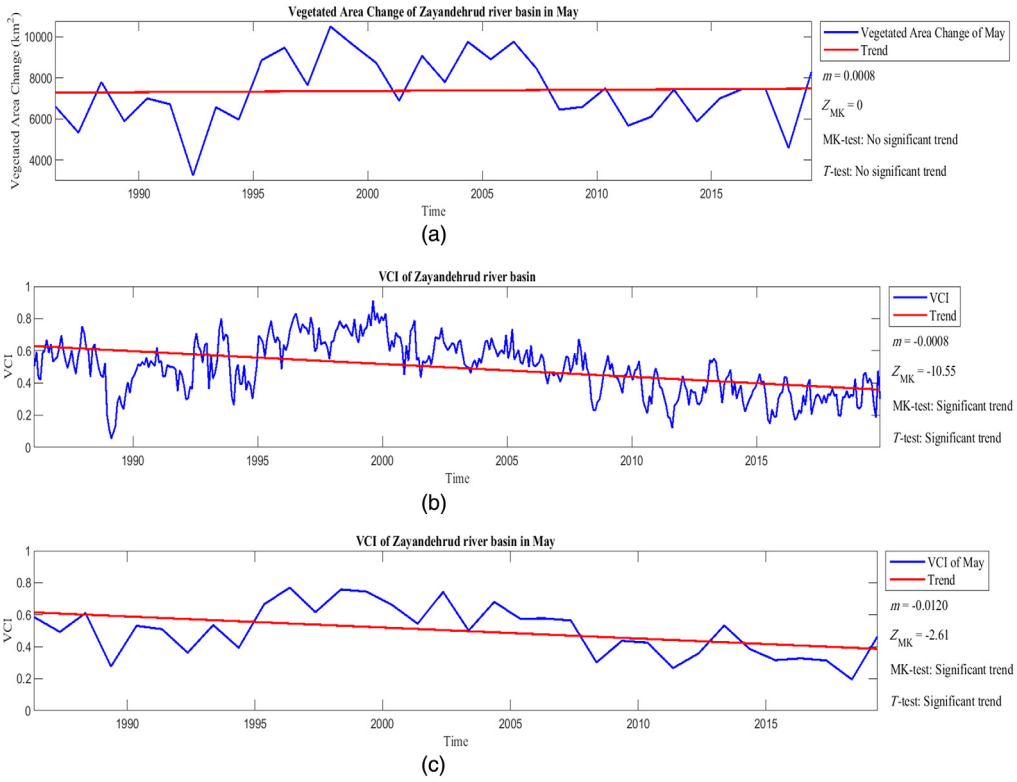

Fig. 5 (a) Vegetated area change in "months May," (b) monthly VCI, and (c) VCI in "months May," calculated in the basin.

maps of the basin for May 2006 and May 2009 are shown in Fig. 6, depicting the nonuniform spatial expansion of the drought in May 2009. Observing different patterns in the VCI maps leads us to investigate the drought pattern distribution in the basin by assessing the drought indices in the sub-basins, where the details of those changes can be studied. The investigation is conducted in the next part of this section.

Finally, to have a comprehensive view of the trends, the slope m of the trends with their associated MK test statistics ZMK values for two scenarios of "all months" and "months May" for different timespans of 1, 3, 6, 9, and 12-month are estimated. The trend line slope values m for drought indices are tabulated in Table 5. If based on ZMK ($|\text{ZMK}| > 1.96$) and t-test, significant trend line slopes are detected in each case, its corresponding cell is boldfaced.

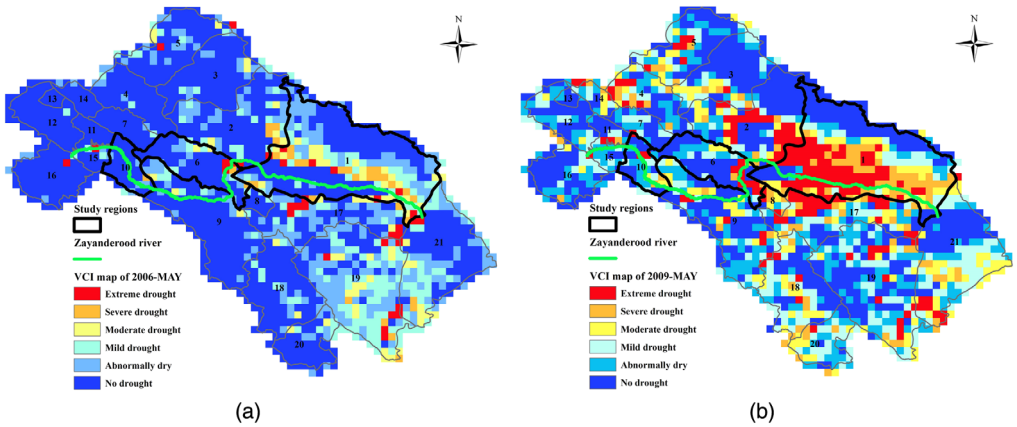

Fig. 6 VCI change maps in May of (a) 2006 and (b) 2009 in the river basin. The maps were produced through using NDVI from NOAA CDR of AVHRR with the spatial resolution of 0.05 deg (~5 km).

Table 5 Trend line slopes (m) and their associated MK test scores (Z_{MK}) of drought indices for two scenarios of "all months" and "months May" and for different timespans (1, 3, 6, 9, and 12 months). The boldface indicate significant trends based on MK and t-test statistics.

	Index	1 month	3 months	6 months	9 months	12 months
Meteorological drought indices	SPI	$m = 0$	$m = 0$	$m = 0$	$m = -0.0001$	$\mathbf{m = -0.0002}$
		$Z_{MK} = 0.41$	$Z_{MK} = 0.23$	$Z_{MK} = -0.13$	$Z_{MK} = -1.52$	$\mathbf{Z_{MK} = -2.01}$
	SPI-May	$m = 0.0049$	$m = -0.0030$	$m = -0.0071$	$m = -0.0025$	$m = -0.0028$
		$Z_{MK} = 1.01$	$Z_{MK} = -0.50$	$Z_{MK} = -1.30$	$Z_{MK} = -0.65$	$Z_{MK} = -0.77$
	SPEI	$\mathbf{m = -0.0005}$	$\mathbf{m = -0.0006}$	$\mathbf{m = -0.0007}$	$\mathbf{m = -0.0009}$	$\mathbf{m = -0.0010}$
		$\mathbf{Z_{MK} = -5.74}$	$\mathbf{Z_{MK} = -7.12}$	$\mathbf{Z_{MK} = -8.34}$	$\mathbf{Z_{MK} = -10}$	$\mathbf{Z_{MK} = -11.26}$
	SPEI-May	$m = 0.0002$	$\mathbf{m = -0.0096}$	$\mathbf{m = -0.0139}$	$\mathbf{m = -0.0117}$	$\mathbf{m = -0.0141}$
		$Z_{MK} = 0$	$\mathbf{Z_{MK} = -2.46}$	$\mathbf{Z_{MK} = -3.05}$	$\mathbf{Z_{MK} = -2.52}$	$\mathbf{Z_{MK} = -3.23}$
	STI	$\mathbf{m = 0.0008}$	$\mathbf{m = 0.0011}$	$\mathbf{m = 0.0013}$	$\mathbf{m = 0.0015}$	$\mathbf{m = 0.0015}$
		$\mathbf{Z_{MK} = 8.32}$	$\mathbf{Z_{MK} = 12.01}$	$\mathbf{Z_{MK} = 15.05}$	$\mathbf{Z_{MK} = 16.66}$	$\mathbf{Z_{MK} = 17.91}$
	STI-May	$\mathbf{m = 0.0094}$	$\mathbf{m = 0.0161}$	$\mathbf{m = 0.0190}$	$\mathbf{m = 0.0211}$	$\mathbf{m = 0.0228}$
		$\mathbf{Z_{MK} = 2.49}$	$\mathbf{Z_{MK} = 4.30}$	$\mathbf{Z_{MK} = 4.39}$	$\mathbf{Z_{MK} = 4.54}$	$\mathbf{Z_{MK} = 4.95}$
Hydrological drought	SWEI-May	$m = -0.0019$	$m = -0.0027$	$m = -0.0027$	$m = -0.0027$	$m = -0.0027$
		$Z_{MK} = -0.74$	$Z_{MK} = -1.01$	$Z_{MK} = -1.01$	$Z_{MK} = -1.01$	$Z_{MK} = -1.01$
	GRACE-DSI	$\mathbf{m = -0.0040}$ $\mathbf{Z_{MK} = -15.40}$	—	—	—	—
	GRACE-DSI-May	$\mathbf{m = -0.0544}$ $\mathbf{Z_{MK} = -4.09}$	—	—	—	—
Agricultural drought	Vegetated area change-May	$m = 0.0008$ $Z_{MK} = 0$	—	—	—	—
	VCI	$\mathbf{m = -0.0008}$ $\mathbf{Z_{MK} = -10.55}$	—	—	—	—
	VCI-May	$\mathbf{m = -0.0120}$ $\mathbf{Z_{MK} = -2.61}$	—	—	—	—

As it is clear from the table, SPEI, GRACE-DSI, and VCI show negative trends, whereas STI has positive trend in the basin for both "all months" as well as "months May" scenarios. On the other hand, SPI, SWEI, and vegetated area change do not show significant trends.

In general, the results of this section indicate that precipitation or snow reserves may not be the driving force for long-term vegetation drought observed in the basin. However, based on STI, the near-surface temperature of the study area has risen which can be one of the reasons for vegetation drought observation. On the other hand, the SPEI, and in particular, GRACE-DSI, shows significant descending trend. This fact can be the results of both increased near-surface temperature and irrigated area expansion in the basin, although the vegetated area change in the whole basin does not show a significant trend. The observation of the significant descending trend of monthly VCI and VCI in "months May," as an indicator of agricultural drought, while no noticeable changes in the vegetated area of the whole river basin is seen, leads our research to bring the study of sub-basins in the focus of the investigation. That is, in particular, from the fact that the Zayandehrud River is an important source for irrigated agriculture in all its three parts: upstream, middle-stream, and downstream sub-basins. We expect that those details can help us to detect the drought drivers in the basin.

4.2 *Drought Analysis of Zayandehrud River Sub-basins*

4.2.1 *Meteorological drought*

For monitoring meteorological drought in the sub-basins, SPI, SPEI, and STI for two scenarios of "all months" and "months May" and for different timespans are used where their slope (m) of the trend lines and their associated Z_{MK} values are calculated in three selected sub-basins 10, 6 and 1. If significant trends based on Z_{MK} and t-test are detected for each case, its corresponding cell is boldfaced. The results of meteorological drought indices are presented in Table 6. In this table, there is just one inconsistency between Z_{MK} and t-test result from SPI-9 of sub-basin 6 (Z_{MK} passed the test whereas t-test does not pass) where the associated cell is specified in hachure. The inconsistency, however, can be considered negligible since the trend line slope is low ($m = 0.0002$).

As it is seen in Table 6 for the monthly SPI, only the trends of SPI-9 and SPI-12 are recognized as significant where the trend slopes are near zero. Those results are consistent in all three sub-basins. SPI trends in "months May" show no significance in any timespan. The results of SPI for all three sub-basins are very similar to each other and consistent with the results of the whole basin (Table 5). This fact indicates the precipitation trend is not much different in different sub-basins, although it should be emphasized that the precipitation in the upstream part of the basin has much more importance than the other parts, since that is by far the most important source of water input into the basin. In the case of SPEI, negative trends are detected in both scenarios for all timespans and in all three sub-basins (except for SPEI-1 in "months May" scenario), which is similar to the results of the basin as a whole. Monthly STI shows significant trends with positive slopes in all three sub-basins and for both scenarios, which can be considered as one of the main reasons for SPEI descending trend. Finally, it can be inferred that the meteorological drought indices are in general very consistent in all three selected sub-basins.

4.2.2 *Hydrological drought*

To monitor hydrological drought in our selected three sub-basins, we use SWEI in "months May" for different timespans, monthly GRACE-DSI and GRACE-DSI in "months May." The line slope (m) of the trends and their associated Z_{MK} values are calculated for the indices in all three sub-basins (Table 7). As it is clear from Table 7, similar to the results of the whole river basin, the trends are not recognized as significant for SWEI in "months May," while we detect negative trend for monthly GRACE-DSI and GRACE-DSI in "months May" in all three sub-basins. As a result, similar to the meteorological drought, the hydrological drought indices show very similar trends in all three sub-basins.

Table 6 Trend line slopes (m) and their associated MK test scores (Z_M) of meteorological drought indices for two scenarios of "all months" and "months May" and for different timespans (1, 3, 6, 9, and 12 months) in three selected sub-basins. The boldface cells indicate significant trends based on MK and t-test statistics.

		Index	1 month	3 months	6 months	9 months	12 months
Meteorological drought indices	Sub-basin 10	SPI	$m = 0.0001$	$m = 0$	$m = 0$	$\mathbf{m = -0.0002}$	$\mathbf{m = -0.0002}$
			$Z_{MK} = 0.54$	$Z_{MK} = 0.28$	$Z_{MK} = -0.73$	$\mathbf{Z_{MK} = -2.19}$	$\mathbf{Z_{MK} = -2.80}$
		SPI-May	$m = 0.0036$	$m = -0.0052$	$m = -0.0054$	$m = -0.0030$	$m = -0.0031$
			$Z_{MK} = 0.86$	$Z_{MK} = -1.48$	$Z_{MK} = -1.48$	$Z_{MK} = -0.98$	$Z_{MK} = -1.13$
		SPEI	$\mathbf{m = -0.0005}$	$\mathbf{m = -0.0006}$	$\mathbf{m = -0.0006}$	$\mathbf{m = -0.0008}$	$\mathbf{m = -0.0009}$
			$\mathbf{Z_{MK} = -5.22}$	$\mathbf{Z_{MK} = -6.29}$	$\mathbf{Z_{MK} = -6.99}$	$\mathbf{Z_{MK} = -8.58}$	$\mathbf{Z_{MK} = -10.12}$
		SPEI-May	$m = -0.0003$	$\mathbf{m = -0.0113}$	$\mathbf{m = -0.0119}$	$\mathbf{m = -0.0096}$	$\mathbf{m = -0.0110}$
			$Z_{MK} = -0.06$	$\mathbf{Z_{MK} = -3.08}$	$\mathbf{Z_{MK} = -2.76}$	$\mathbf{Z_{MK} = -2.70}$	$\mathbf{Z_{MK} = -2.99}$
		STI	$\mathbf{m = 0.0010}$	$\mathbf{m = 0.0012}$	$\mathbf{m = 0.0014}$	$\mathbf{m = 0.0015}$	$\mathbf{m = 0.0016}$
			$\mathbf{Z_{MK} = 10.40}$	$\mathbf{Z_{MK} = 14.02}$	$\mathbf{Z_{MK} = 16.72}$	$\mathbf{Z_{MK} = 17.62}$	$\mathbf{Z_{MK} = 18.85}$
		STI-May	$\mathbf{m = 0.0120}$	$\mathbf{m = 0.0163}$	$\mathbf{m = 0.0185}$	$\mathbf{m = 0.0188}$	$\mathbf{m = 0.0193}$
			$\mathbf{Z_{MK} = 2.55}$	$\mathbf{Z_{MK} = 4.54}$	$\mathbf{Z_{MK} = 4.89}$	$\mathbf{Z_{MK} = 4.77}$	$\mathbf{Z_{MK} = 5.31}$

Table 6 (*Continued*).

	Index	1 month	3 months	6 months	9 months	12 months
Sub-basin 6	SPI	$m = 0.0001$	$m = 0$	$m = 0$	$m = -0.0002$	$\mathbf{m = -0.0002}$
		$Z_{MK} = 0.53$	$Z_{MK} = 0.21$	$Z_{MK} = -0.47$	$Z_{MK} = -2.10$	$\mathbf{Z_{MK} = -2.69}$
	SPI-May	$m = 0.0045$	$m = -0.0034$	$m = -0.0062$	$m = -0.0029$	$m = -0.0033$
		$Z_{MK} = 1.19$	$Z_{MK} = -0.62$	$Z_{MK} = -1.33$	$Z_{MK} = -0.95$	$Z_{MK} = -0.89$
	SPEI	$\mathbf{m = -0.0005}$	$\mathbf{m = -0.0006}$	$\mathbf{m = -0.0007}$	$\mathbf{m = -0.0009}$	$\mathbf{m = -0.0010}$
		$\mathbf{Z_{MK} = -5.24}$	$\mathbf{Z_{MK} = -6.60}$	$\mathbf{Z_{MK} = -7.77}$	$\mathbf{Z_{MK} = -9.55}$	$\mathbf{Z_{MK} = -10.77}$
	SPEI-May	$m = -0.0004$	$\mathbf{m = -0.0100}$	$\mathbf{m = -0.0124}$	$\mathbf{m = -0.0103}$	$\mathbf{m = -0.0126}$
		$Z_{MK} = -0.33$	$\mathbf{Z_{MK} = -2.46}$	$\mathbf{Z_{MK} = -2.91}$	$\mathbf{Z_{MK} = -2.64}$	$\mathbf{Z_{MK} = -3.11}$
	STI	$\mathbf{m = 0.0008}$	$\mathbf{m = 0.0011}$	$\mathbf{m = 0.0013}$	$\mathbf{m = 0.0015}$	$\mathbf{m = 0.0015}$
		$\mathbf{Z_{MK} = 8.90}$	$\mathbf{Z_{MK} = 12.44}$	$\mathbf{Z_{MK} = 15.43}$	$\mathbf{Z_{MK} = 16.91}$	$\mathbf{Z_{MK} = 18.23}$
	STI-May	$\mathbf{m = 0.0110}$	$\mathbf{m = 0.0162}$	$\mathbf{m = 0.0178}$	$\mathbf{m = 0.0178}$	$\mathbf{m = 0.0193}$
		$\mathbf{Z_{MK} = 2.61}$	$\mathbf{Z_{MK} = 4.24}$	$\mathbf{Z_{MK} = 4.42}$	$\mathbf{Z_{MK} = 4.65}$	$\mathbf{Z_{MK} = 5.10}$

Table 6 (*Continued*).

	Index	1 month	3 months	6 months	9 months	12 months
Sub-basin 1	SPI	$m = 0$	$m = -0.0001$	$m = -0.0001$	$\mathbf{m = -0.0002}$	$\mathbf{m = -0.0003}$
		$Z_{MK} = 0.05$	$Z_{MK} = -0.50$	$Z_{MK} = -0.73$	$\mathbf{Z_{MK} = -2.24}$	$\mathbf{Z_{MK} = -2.63}$
	SPI-May	$m = 0.0033$	$m = -0.0037$	$m = -0.0072$	$m = -0.0035$	$m = -0.0039$
		$Z_{MK} = 0.65$	$Z_{MK} = -0.56$	$Z_{MK} = -1.57$	$Z_{MK} = -0.68$	$Z_{MK} = -0.92$
	SPEI	$\mathbf{m = -0.0005}$	$\mathbf{m = -0.0006}$	$\mathbf{m = -0.0008}$	$\mathbf{m = -0.0010}$	$\mathbf{m = -0.0011}$
		$\mathbf{Z_{MK} = -4.97}$	$\mathbf{Z_{MK} = -6.71}$	$\mathbf{Z_{MK} = -8.77}$	$\mathbf{Z_{MK} = -10.71}$	$\mathbf{Z_{MK} = -11.90}$
	SPEI-May	$m = -0.0011$	$\mathbf{m = -0.0103}$	$\mathbf{m = -0.0134}$	$\mathbf{m = -0.0123}$	$\mathbf{m = -0.0141}$
		$Z_{MK} = -0.18$	$\mathbf{Z_{MK} = -2.49}$	$\mathbf{Z_{MK} = -3.14}$	$\mathbf{Z_{MK} = -2.88}$	$\mathbf{Z_{MK} = -3.41}$
	STI	$\mathbf{m = 0.0007}$	$\mathbf{m = 0.0011}$	$\mathbf{m = 0.0013}$	$\mathbf{m = 0.0014}$	$\mathbf{m = 0.0015}$
		$\mathbf{Z_{MK} = 7.84}$	$\mathbf{Z_{MK} = 11.65}$	$\mathbf{Z_{MK} = 14.62}$	$\mathbf{Z_{MK} = 16.42}$	$\mathbf{Z_{MK} = 17.64}$
	STI-May	$\mathbf{m = 0.0090}$	$\mathbf{m = 0.0155}$	$\mathbf{m = 0.0179}$	$\mathbf{m = 0.0183}$	$\mathbf{m = 0.0187}$
		$Z_{MK} = 2.34$	$\mathbf{Z_{MK} = 4.15}$	$\mathbf{Z_{MK} = 4.24}$	$\mathbf{Z_{MK} = 4.39}$	$\mathbf{Z_{MK} = 4.71}$

Table 7 Trend line slopes (m) and their associated MK test scores (Z_{MK}) of hydrological drought indices for two scenarios of "all months" and "months May" and for different timespans (1, 3, 6, 9, and 12 months) in three selected sub-basins. The boldfaced cells indicate significant trends based on MK and t-test statistics.

		Index	1 month	3 months	6 months	9 months	12 months
Hydrological drought	Sub-basin 10	SWEI-May	$m = -0.0004$	$m = -0.0009$	$m = -0.0009$	$m = -0.0009$	$m = -0.0009$
			$Z_{MK} = -0.18$	$Z_{MK} = -0.42$	$Z_{MK} = -0.42$	$Z_{MK} = -0.42$	$Z_{MK} = -0.42$
		GRACE-DSI	**$m = -0.0041$** **$Z_{MK} = -16.48$**	—	—	—	—
		GRACE-DSI-May	**$m = -0.0558$** **$Z_{MK} = -4.55$**	—	—	—	—
	Sub-basin 6	SWEI-May	$m = -0.0002$	$m = -0.0014$	$m = -0.0014$	$m = -0.0014$	$m = -0.0014$
			$Z_{MK} = -0.47$	$Z_{MK} = -0.83$	$Z_{MK} = -0.83$	$Z_{MK} = -0.83$	$Z_{MK} = -0.83$
		GRACE-DSI	**$m = -0.0041$** **$Z_{MK} = -16.48$**	—	—	—	—
		GRACE-DSI-May	**$m = -0.0558$** **$Z_{MK} = -4.55$**	—	—	—	—
	Sub-basin 1	SWEI-May	$m = -0.0018$	$m = -0.0030$	$m = -0.0030$	$m = -0.0030$	$m = -0.0030$
			$Z_{MK} = -0.98$	$Z_{MK} = -1.33$	$Z_{MK} = -1.33$	$Z_{MK} = -1.33$	$Z_{MK} = -1.33$
		GRACE-DSI	**$m = -0.0041$** **$Z_{MK} = -16.48$**	—	—	—	—
		GRACE-DSI-May	**$m = -0.0558$** **$Z_{MK} = -4.55$**	—	—	—	—

It should be also mentioned that the spatial resolution of the GRACE data is not sufficient for detailed study of the sub-basins, even though the JPL Mascon Level 3 of the GRACE makes use the hydrological models to provide 0.5 deg × 0.5 deg space resolution for the TWS change.

Moreover, we assess the water area changes at three spots: (i) behind the Zayandehrud River dam (Zayandehrud Lake), (ii) in Fakhrabad as an area in sub-basin 6 midway between the river sources and Gavkhuni Wetland, and (iii) in Gavkhuni Wetland itself as the endpoint of the river. In this way, monthly NDWI is calculated for these three parts of Zayandehrud River, using of Landsat images. To remove the cloud effect, we exclude all the images with cloudy pixels, even if only one pixel is contaminated. Afterward, for estimating water pixels, a threshold of 0.08 based on experiments is applied on NDWI values, where the pixels with the values greater than the threshold are considered as water pixels. The time series of water area change in the three selected areas are shown in Fig. 7. As results show, the water area behind the Zayandehrud River dam has some fluctuations after its first severe reduction of water area in 2000, while the area is near normal between the years 2002 to 2007. After this period, a descending trend can be seen in the time series. On the other hand, after 2000, the water area in Fakhrabad was zero or near zero in most of the time. More interestingly, since that time, the water area in Gavkhuni Wetland has been decreased to near zero and never reached to its normal level. The results clearly demonstrate that no causal relationship is seen between the amounts of water area in Zayandehrud River dam, Fakhrabad area, and in particular Gavkhuni Wetland. This fact is of special interest since the water area behind the Zayandehrud River dam has been near to its normal in some years after 2000. The potential explanation for this observation comes from the fact that during this period, the agricultural fields in the upstream parts of the river may have been expanded. That is clearly seen in the sub-basin 10, as an example of the next section.

To evaluate the groundwater level fluctuation, we use groundwater depletion rate for each aquifer as complementary information for our analysis. The time series of the ground water

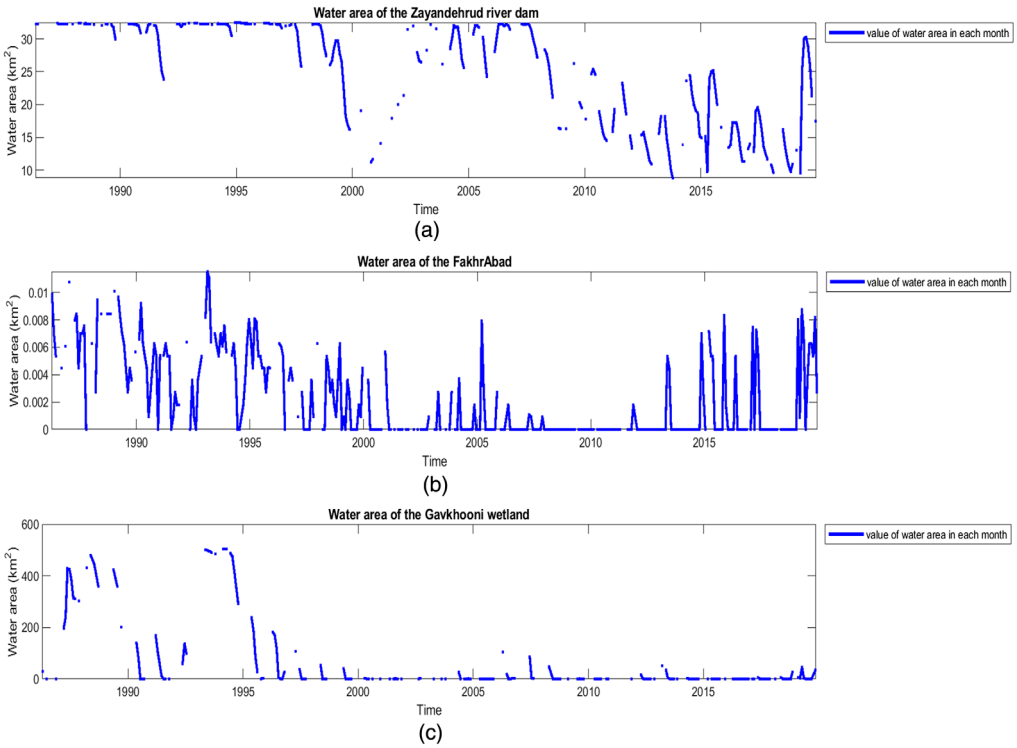

Fig. 7 Time series of water area change in (a) Zayandehrud River dam, (b) FakhAbad area, and (c) Gavkhuni Wetland in the period of 2010 to 2019. The product was estimated using Landsat images with the spatial resolution of 30 m.

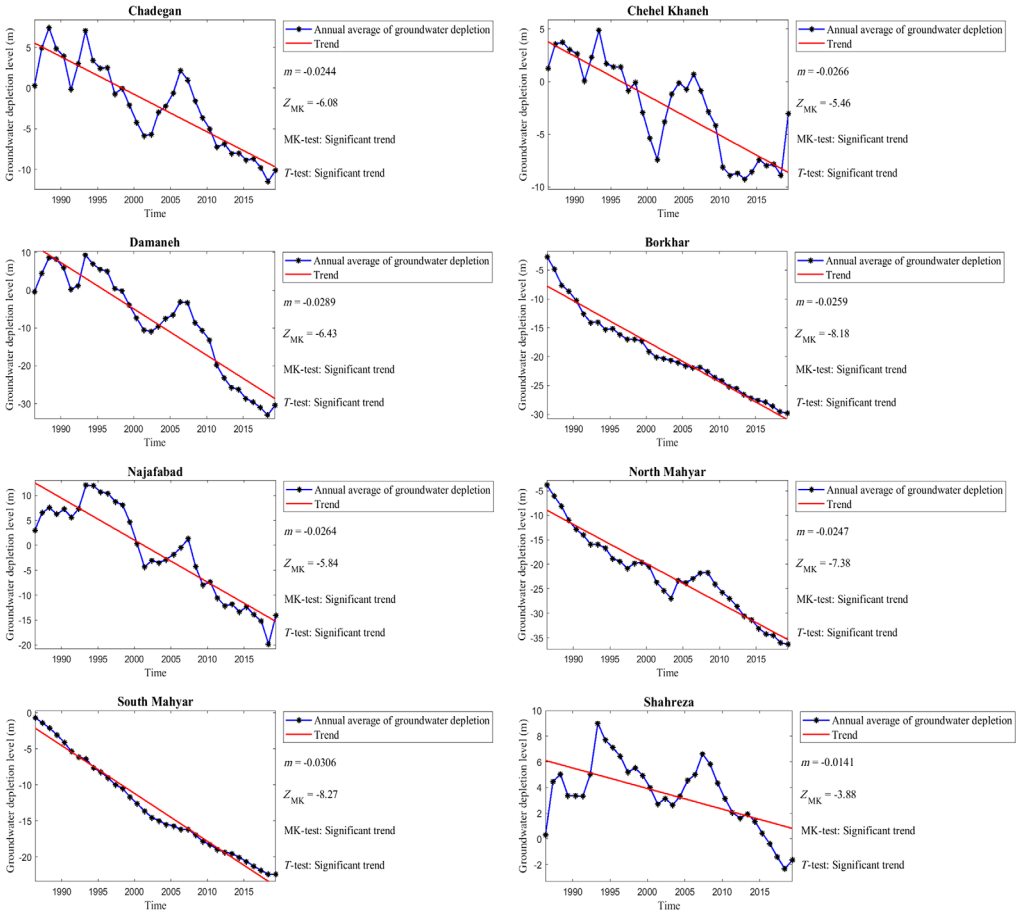

Fig. 8 Groundwater depletion rate in eight aquifers located in the basin in the period of 2010 to 2019.

depletion for eight aquifers in the basin are shown in Fig. 8. Chadegan, Chehel Khaneh, and Dameneh aquifers are located in the upstream, whereas Brokhar, Najafabad, and North Mahyar are located in the midstream, and South Mahyar and Shahreza are within in the downstream parts of the basin. Although these eight aquifers are scattered in three parts of the basin, no significant differences are observed in their groundwater depletion trend. The results show that the groundwater in all three parts of the river basin has very significant descending trend, which is in agreement with the GRACE-DSI results.

4.2.3 *Agricultural drought*

For the assessment of agricultural drought indices in the selected sub-basins, the line slope (m) of the trends and the associated Z_{MK} values of the vegetated area change in "months May," monthly VCI and VCI in "months May" are calculated for three sub-basins of interest (Table 8). The results of the MK test as well as the t-test show that the vegetated area change, monthly VCI and VCI in "months May" have positive trends in sub-basin 10, whereas the indices in two other sub-basins 6 and 1 show negative slopes. The time series of VCI and vegetated area change in "months May" for three sub-basins are also shown in Fig. 9.

To bring a few examples of the VCI spatial distribution in "months May," as an important growth period, of the last decade, the VCI maps in the period of 2010 to 2019 are shown in Fig. 10. As the results show, although the midstream and downstream areas of the basin are mostly affected by agricultural drought, the upstream areas remain in an almost stable good condition.

Table 8 Trend line slopes (m) and the associated MK test scores (Z_{MK}) of agricultural drought indices for two scenarios of "all months" and "months May" in three sub-basins. The boldface cells indicate significant trends based on MK and t-test statistics.

		Index	1 month
Agricultural drought	Sub-basin 10	Vegetated area change-May	$\mathbf{m = 0.0237}$
			$\mathbf{Z_{MK} = 5.59}$
		VCI	$\mathbf{m = 0.0007}$
			$\mathbf{Z_{MK} = 8.93}$
		VCI-May	$\mathbf{m = 0.0173}$
			$\mathbf{Z_{MK} = 4.89}$
	Sub-basin 6	Vegetated area change-May	$\mathbf{m = -0.0134}$
			$\mathbf{Z_{MK} = -3.91}$
		VCI	$\mathbf{m = -0.0009}$
			$\mathbf{Z_{MK} = -11.95}$
		VCI-May	$\mathbf{m = -0.0139}$
			$\mathbf{Z_{MK} = -3.71}$
	Sub-basin 1	Vegetated area change-May	$\mathbf{m = -0.0184}$
			$\mathbf{Z_{MK} = -2.46}$
		VCI	$\mathbf{m = -0.0008}$
			$\mathbf{Z_{MK} = -11.01}$
		VCI-May	$\mathbf{m = -0.0115}$
			$\mathbf{Z_{MK} = -2.58}$

5 Summary and Conclusion

This research work aimed to study the long-term drought condition of the Zayandehrud River basin in central Iran. The work employed meteorological drought indices (SPI, SPEI, and STI), hydrological drought indices (SWEI, NDWI, and GRACE-DSI), and a vegetation (agricultural) drought index (VCI) from 1986 to 2019, where the long-term trend of the aforementioned indices were analyzed.

Inspecting the results from our trend analysis of different indices in the river basin as well as its sub-basins may bring us to an important conclusive point. While the long-term precipitation index and snow reserves do not show a trend during the study period, we observe rising air temperature index and falling GRACE-DSI and groundwater storage in the river basin and all three selected sub-basins of the study region. On the other hand, the agricultural conditions in the upstream, midstream, and downstream parts of the basin show different spatial patterns. We also observe that almost no water has reached Fakhrabad area and Gavkhuni Wetland after the year 2000, even though we see significant fluctuations in the water area of the Zayandehrud dam in the recent years. The plausible explanation for this observation is that the expansion of the agricultural fields in the river upstream as well as rising air temperature and increasing population and industrial activities in the basin are most likely the driving forces for agricultural drought intensification in the midstream and downstream parts of the basin. Knowing that the basin imports water from the neighboring catchment "Karun" through transbasin diversion tunnels, although part of the water is transferred to the cities outside the basin, also signifies the remarkable water consumption in the region during recent decades.

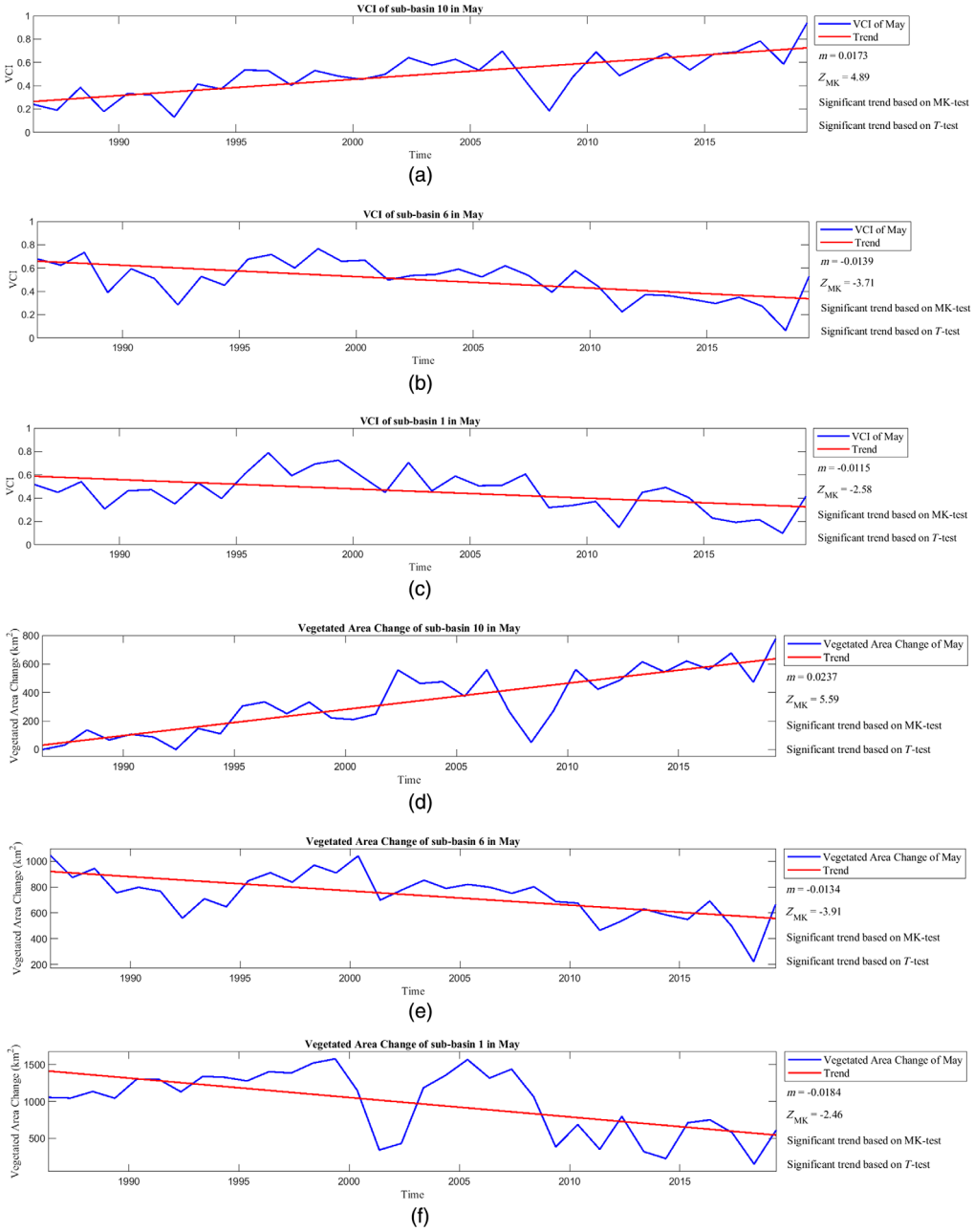

Fig. 9 VCI "months May" for (a) sub-basin 10, (b) sub-basin 6, and (c) sub-basin 1 and the vegetated area change in "months May" for (d) sub-basin 10, (e) sub-basin 6, and (f) sub-basin 1.

The small negative trend of SPEI in the river basin and its different sub-basin can be interpreted as the result of either temperature increase or agricultural expansion in different regions of the study area or the combination of both effects. It is important to mention that although SPEI is a meteorological index, it can also be affected by agricultural activities where the evapotranspiration from the vegetation can influence the index value.

Another important issue to be mentioned is that the trend slope of SPEI is not significant enough to explain the weighty negative trend of GRACE-DSI, the noticeable decline in the groundwater level of the piezometric wells, and the almost-zero surface water area in the Gavkhuni Wetland. On the contrary, those remarkable losses in the surface water and groundwater storage may be better explained by the increase of water consumptions, mainly for the agricultural activities in the upstream (as seen through the vegetated area expansion and VCI) as well as the rise of water use by the industry and the urban expansion during the study period.

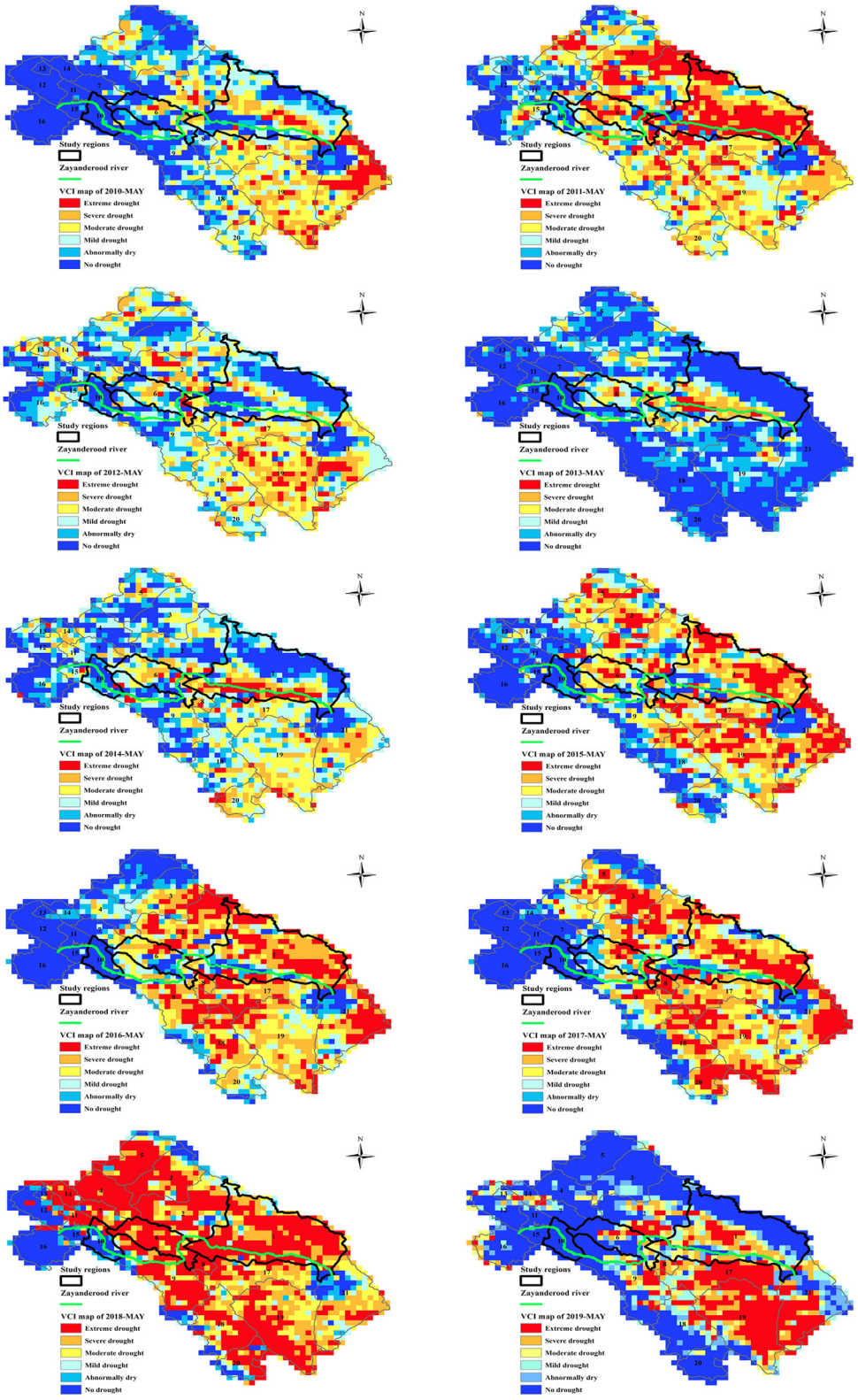

Fig. 10 Selected VCI maps of the basin in the period of 2010 to 2019 for the "months May." The maps were produced through using NDVI from NOAA CDR of AVHRR with the spatial resolution of 0.05 deg (~5 km).

To summarize the findings of our current study, we clearly showed the impact of human activities, in particular the agricultural expansion in the river upstream, on the drought condition of the midstream and downstream, although the influence of water consumption by expanding industry and population growth as well as the rising air temperature should be also considered. To be more specific, depicted in the water level time-series of the piezometric wells and GRACE-DSI, we observed overextraction of groundwater for human activities in the whole river basin. Furthermore, through looking into the time-series of NDWI at different places along the river, we noticed excessive water withdrawal in the river upstream. These results are in agreement with the outputs of several other studies in different areas across the globe, a few of them cited in the literature review of this study, where human activities have been recognized as the main drivers for the agricultural drought in the downstream.

The focus of this research work was to investigate the long-term drought condition of the river basin through different drought indices and information. Here, we did not look into the specific years when the drought happened. Obviously, it would be of great interest to analyze the datasets for more detailed study of the drought events within the study period of our work. In particular, identifying the drought events as well as their intensities might be of an interest. One can also think of different methodologies for extraction of trend and periodic signal features. Among those methodologies are obviously the nonstationary signal processing algorithms where the frequency change of the drought characteristics can be identified and analyzed in detail.

Acknowledgments

The authors would like to take this opportunity to sincerely thank the Google Earth Engine team for providing free access to part of datasets of this study. We would also like to thank the Google Collaboratory team for providing free cloud-computing resources, used in our research work. This work was partly funded by the German Federal Ministry of Education and Research (BMBF) in the framework of the international future AI lab "AI4EO – Artificial Intelligence for Earth Observation: Reasoning, Uncertainties, Ethics and Beyond" (Grant No. 01DD20001).

References

1. G. Hagman et al., *Prevention Better Than Cure. Report on Human and Environmental Disasters in the Third World*, Vol. **2**, Swedish Red Cross (1984).
2. L. Zhang et al., "Studying drought phenomena in the Continental United States in 2011 and 2012 using various drought indices," *Remote Sens. Environ.* **190**, 96–106 (2017).
3. B. Lloyd-Hughes, "The impracticality of a universal drought definition," *Theor. Appl. Climatol.* **117**(3-4), 607–611 (2014).
4. H. West, N. Quinn, and M. Horswell, "Remote sensing for drought monitoring & impact assessment: progress, past challenges and future opportunities," *Remote Sens. Environ.* **232**, 111291 (2019).
5. D. A. Wilhite and M. H. Glantz, "Understanding: the drought phenomenon: the role of definitions," *Water Int.* **10**(3), 111–120 (1985).
6. A. Zhang and G. Jia, "Monitoring meteorological drought in semiarid regions using multi-sensor microwave remote sensing data," *Remote Sens. Environ.* **134**, 12–23 (2013).
7. A. Van Loon, "Hydrological drought explained," *WIRES Water* **2**, 359–392 (2015).
8. X. Liu et al., "Agricultural drought monitoring: progress, challenges, and prospects," *J. Geogr. Sci.* **26**(6), 750–767 (2016).
9. J. A. Keyantash and J. A. Dracup, "An aggregate drought index: assessing drought severity based on fluctuations in the hydrologic cycle and surface water storage," *Water Resour. Res.* **40**(9) (2004).
10. O. V. Wilhelmi and D. A. Wilhite, "Assessing vulnerability to agricultural drought: a Nebraska case study," *Nat. Hazards* **25**(1), 37–58 (2002).
11. L. Huang et al., "A global examination of the response of ecosystem water-use efficiency to drought based on MODIS data," *Sci. Tot. Environ.* **601**, 1097–1107 (2017).

12. A. House, J. Thompson, and M. Acreman, "Projecting impacts of climate change on hydrological conditions and biotic responses in a chalk valley riparian wetland," *J. Hydrol.* **534**, 178–192 (2016).
13. S. Piao et al., "NDVI-based increase in growth of temperate grasslands and its responses to climate changes in China," *Global Environ. Change* **16**(4), 340–348 (2006).
14. J. M. Stribling and J. C. Cornwell, "Nitrogen, phosphorus, and sulfur dynamics in a low salinity marsh system dominated by *Spartina alterniflora*," *Wetlands* **21**(4), 629–638 (2001).
15. C. Gouveia et al., "Drought impacts on vegetation activity in the Mediterranean region: an assessment using remote sensing data and multi-scale drought indicators," *Global Planet. Change* **151**, 15–27 (2017).
16. K. Winkler, U. Gessner, and V. Hochschild, "Identifying droughts affecting agriculture in Africa based on remote sensing time series between 2000–2016: rainfall anomalies and vegetation condition in the context of ENSO," *Remote Sens.* **9**(8), 831 (2017).
17. D. A. Mariano et al., "Use of remote sensing indicators to assess effects of drought and human-induced land degradation on ecosystem health in northeastern Brazil," *Remote Sens. Environ.* **213**, 129–143 (2018).
18. F. Satgé et al., "Role of climate variability and human activity on Poopó Lake droughts between 1990 and 2015 assessed using remote sensing data," *Remote Sens.* **9**(3), 218 (2017).
19. B. Khazaei et al., "Climatic or regionally induced by humans? Tracing hydro-climatic and land-use changes to better understand the Lake Urmia tragedy," *J. Hydrol.* **569**, 203–217 (2019).
20. K. Madani, A. AghaKouchak, and A. Mirchi, "Iran's socio-economic drought: challenges of a water-bankrupt nation," *Iranian Stud.* **49**(6), 997–1016 (2016).
21. A. M. Al-Damkhi, S. Abdul-Wahab, and A. Al-Nafisi, "On the need to reconsider water management in Kuwait," *Clean Technol. Environ. Policy* **11**(4), 379 (2009).
22. H. B. Abarghouei et al., "The survey of climatic drought trend in Iran," *Stochast. Environ. Res. Risk Assess.* **25**(6), 851 (2011).
23. R. Berndtsson et al., "Traditional irrigation techniques in MENA with a focus on Tunisia," *Hydrol. Sci. J.* **61**(7), 1346–1357 (2016).
24. R. Davtalab et al., "Improving continuous hydrologic modeling of data-poor river basins using hydrologic engineering center's hydrologic modeling system: case study of Karkheh River basin," *J. Hydrol. Eng.* **22**(8), 05017011 (2017).
25. A. Gohari et al., "Water transfer as a solution to water shortage: a fix that can backfire," *J. Hydrol.* **491**, 23–39 (2013).
26. S. Golian, O. Mazdiyasni, and A. AghaKouchak, "Trends in meteorological and agricultural droughts in Iran," *Theor. Appl. Climatol.* **119**(3-4), 679–688 (2015).
27. H. Hashemi, "Climate change and the future of water management in Iran," *Middle East Critiq.* **24**(3), 307–323 (2015).
28. A. Mehran, O. Mazdiyasni, and A. AghaKouchak, "A hybrid framework for assessing socioeconomic drought: linking climate variability, local resilience, and demand," *J. Geophys. Res.: Atmos.* **120**(15), 7520–7533 (2015).
29. M. Tourian et al., "A spaceborne multisensor approach to monitor the desiccation of Lake Urmia in Iran," *Remote Sens. Environ.* **156**, 349–360 (2015).
30. P. Saemian et al., "Analyzing the Lake Urmia restoration progress using ground-based and spaceborne observations," *Sci. Tot. Environ.* **739**, 139857 (2020).
31. A. F. Van Loon et al., "Drought in the anthropocene," *Nat. Geosci.* **9**(2), 89–91 (2016).
32. A. F. Van Loon et al., "Drought in a human-modified world: reframing drought definitions, understanding, and analysis approaches," *Hydrol. Earth Syst. Sci.* **20**, 3631–3650 (2016).
33. S. Rangecroft et al., "An observation-based method to quantify the human influence on hydrological drought: upstream–downstream comparison," *Hydrol. Sci. J.* **64**(3), 276–287 (2019).
34. E. Tavazohi and M. A. Nadoushan, "Assessment of drought in the Zayandehroud Basin during 2000–2015 using NDDI and SPI indices," *Fresenius Environ. Bull.* **27**(4), 2332–2340 (2018).
35. H. R. Safavi et al., "A new hybrid drought-monitoring framework based on nonparametric standardized indicators," *Hydrol. Res.* **49**(1), 222–236 (2018).

36. A. Farahmand and A. AghaKouchak, "A generalized framework for deriving nonparametric standardized drought indicators," *Adv. Water Resour.* **76**, 140–145 (2015).
37. M. Arast et al., "Assessment of groundwater level variations in different land-uses using GRACE satellite data (case study: Zayanderud Basin, Iran)," *J. Hydrosci. Environ.* **3**(5), 52–59 (2019).
38. N. Abou Zaki et al., "Evaluating impacts of irrigation and drought on river, groundwater and a terminal wetland in the Zayanderud Basin, Iran," *Water* **12**(5), 1302 (2020).
39. M. Hekmatpanah, M. Nasri, and F. S. Sardu, "Effect of industrial and agricultural pollutants on the sustainability of Gavkhuni lagoon wetland ecosystem," *Afr. J. Agric. Res.* **7**(20), 3049–3059 (2012).
40. M. Akbari et al., "Monitoring irrigation performance in Esfahan, Iran, using NOAA satellite imagery," *Agric. Water Manage.* **88**(1–3), 99–109 (2007).
41. H. R. Safavi, M. H. Golmohammadi, and S. Sandoval-Solis, "Expert knowledge based modeling for integrated water resources planning and management in the Zayandehrud River Basin," *J. Hydrol.* **528**, 773–789 (2015).
42. S. Javadinejad, K. Ostad-Ali-Askari, and S. Eslamian, "Application of multi-index decision analysis to management scenarios considering climate change prediction in the Zayandeh Rud River Basin," *Water Conserv. Sci. Eng.* **4**(1), 53–70 (2019).
43. K. Madani and M. A. Mariño, "System dynamics analysis for managing Iran's Zayandeh-Rud river basin," *Water Resour. Manage.* **23**(11), 2163–2187 (2009).
44. F. Molle, I. Ghazi, and H. Murray-Rust, "Buying respite: Esfahan and the Zayandeh Rud river basin, Iran," *River Basin Trajectories: Societies, Environments and Development*, Vol. **196**, F. Molle and P. Wester, Eds., International Water Management Institute (IWMI) (2009).
45. M. Bijani and D. Hayati, "Farmers' perceptions toward agricultural water conflict: the case of Doroodzan dam irrigation network, Iran," *J. Agric. Sci. Technol. (JAST)* **17**(3), 561–575 (2015).
46. H. Hersbach et al., "The ERA5 global reanalysis," *Q. J. R. Meteorol. Soc.* **146**(730), 1999–2049 (2020).
47. H. Hersbach et al., "Global reanalysis: goodbye ERA-Interim, hello ERA5," *ECMWF Newslett.* **159**, 17–24 (2019).
48. J. Muñoz Sabater, "ERA5-Land monthly averaged data from 1981 to present. Copernicus Climate Change Service (C3S) Climate Data Store (CDS)," (2019), https://cds.climate.copernicus.eu/cdsapp#!/dataset/reanalysis-era5-land-monthly-means?tab=overview.
49. A. McNally et al., "A land data assimilation system for sub-Saharan Africa food and water security applications," *Sci. Data* **4**(1), 170012 (2017).
50. C. D. Peters-Lidard et al., "High-performance Earth system modeling with NASA/GSFC's land information system," *Innov. Syst. Software Eng.* **3**(3), 157–165 (2007).
51. C. Funk et al., "The climate hazards infrared precipitation with stations: a new environmental record for monitoring extremes," *Sci. Data* **2**(1), 150066 (2015).
52. B. D. Tapley et al., "GRACE measurements of mass variability in the Earth system," *Science* **305**(5683), 503–505 (2004).
53. J. Wahr et al., "Time-variable gravity from GRACE: first results," *Geophys. Res. Lett.* **31**(11) (2004).
54. E. Vermote, *Program. 2019. NOAA Climate Data Record (CDR) of AVHRR Normalized Difference Vegetation Index (NDVI), Version 5*, NOAA National Centers for Environmental Information (2019).
55. A. Zargar et al., "A review of drought indices," *Environ. Rev.* **19**, 333–349 (2011).
56. M. Zhao, I. Velicogna, and J. S. Kimball, "A global gridded dataset of GRACE drought severity index for 2002–14: comparison with PDSI and SPEI and a case study of the Australia millennium drought," *J. Hydrometeorol.* **18**(8), 2117–2129 (2017).
57. F. N. Kogan, "Remote sensing of weather impacts on vegetation in non-homogeneous areas," *Int. J. Remote Sens.* **11**(8), 1405–1419 (1990).
58. F. N. Kogan, "Application of vegetation index and brightness temperature for drought detection," *Adv. Space Res.* **15**(11), 91–100 (1995).
59. X. Liu et al., "GRACE satellite-based drought index indicating increased impact of drought over major basins in China during 2002–2017," *Agric. For. Meteorol.* **291**, 108057 (2020).

60. C. Bhuiyan, R. Singh, and F. Kogan, "Monitoring drought dynamics in the Aravalli region (India) using different indices based on ground and remote sensing data," *Int. J. Appl. Earth Obs. Geoinf.* **8**(4), 289–302 (2006).
61. F. Zambrano et al., "Sixteen years of agricultural drought assessment of the BioBío region in Chile using a 250 m resolution vegetation condition index (VCI)," *Remote Sens.* **8**(6), 530 (2016).
62. R. P. Singh, S. Roy, and F. Kogan, "Vegetation and temperature condition indices from NOAA AVHRR data for drought monitoring over India," *Int. J. Remote Sens.* **24**(22), 4393–4402 (2003).
63. K. Wang, T. Li, and J. Wei, "Exploring drought conditions in the three river headwaters region from 2002 to 2011 using multiple drought indices," *Water* **11**(2), 190 (2019).
64. S. Chaudhary and A. C. Pandey, "Multiple indices based drought analysis by using long term climatic variables over a part of Koel river basin, India," *Spatial Inf. Res.* **28**, 273–285 (2019).
65. S. Ali et al., "Analysis of vegetation dynamics, drought in relation with climate over South Asia from 1990 to 2011," *Environ. Sci. Pollut. Res.* **26**(11), 11470–11481 (2019).
66. F. Kogan et al., "AVHRR-based spectral vegetation index for quantitative assessment of vegetation state and productivity," *Photogramm. Eng. Remote Sens.* **69**(8), 899–906 (2003).
67. S. M. Quiring, "Developing objective operational definitions for monitoring drought," *J. Appl. Meteorol. Climatol.* **48**(6), 1217–1229 (2009).
68. R. Seiler, M. Hayes, and L. Bressan, "Using the standardized precipitation index for flood risk monitoring," *Int. J. Climatol.: J. R. Meteorol. Soc.* **22**(11), 1365–1376 (2002).
69. Z. Hao and A. AghaKouchak, "A nonparametric multivariate multi-index drought monitoring framework," *J. Hydrometeorol.* **15**(1), 89–101 (2014).
70. I. I. Gringorten, "A plotting rule for extreme probability paper," *J. Geophys. Res.* **68**(3), 813–814 (1963).
71. S. M. Vicente-Serrano, S. Beguería, and J. I. López-Moreno, "A multiscalar drought index sensitive to global warming: the standardized precipitation evapotranspiration index," *J. Clim.* **23**(7), 1696–1718 (2010).
72. M. Svoboda et al., "The drought monitor," *Bull. Am. Meteorol. Soc.* **83**(8), 1181–1190 (2002).
73. S. K. McFeeters, "The use of the normalized difference water index (NDWI) in the delineation of open water features," *Int. J. Remote Sens.* **17**(7), 1425–1432 (1996).
74. V. K. Gautam et al., "Assessment of surface water dynamics in Bangalore using WRI, NDWI, MNDWI, supervised classification and KT transformation," *Aquat. Proc.* **4**, 739–746 (2015).
75. X. Yang et al., "Mapping of urban surface water bodies from Sentinel-2 MSI imagery at 10 m resolution via NDWI-based image sharpening," *Remote Sens.* **9**(6), 596 (2017).
76. E. Özelkan, "Water body detection analysis using NDWI indices derived from landsat-8 OLI," *Pol. J. Environ. Stud.* **29**(2), 1759–1769 (2020).
77. B. L. Welch, "The generalization of student's' problem when several different population variances are involved," *Biometrika* **34**(1/2), 28–35 (1947).
78. M. G. Kendall, *Rank Correlation Methods*, Griffin, Oxford, UK (1948).
79. H. B. Mann, "Nonparametric tests against trend," *Econometrica: J. Econ. Soc.* **13**, 245–259 (1945).
80. S. Yue and P. Pilon, "A comparison of the power of the t test, Mann-Kendall and bootstrap tests for trend detection/Une comparaison de la puissance des tests t de Student, de Mann-Kendall et du bootstrap pour la détection de tendance," *Hydrol. Sci. J.* **49**(1), 21–37 (2004).
81. K.-H. Ahn and V. Merwade, "Quantifying the relative impact of climate and human activities on streamflow," *J. Hydrol.* **515**, 257–266 (2014).
82. M. Masroor et al., "Exploring climate variability and its impact on drought occurrence: evidence from Godavari Middle sub-basin, India," *Weather Clim. Extremes* **30**, 100277 (2020).
83. E. Douglas, R. Vogel, and C. Kroll, "Trends in floods and low flows in the United States: impact of spatial correlation," *J. Hydrol.* **240**(1-2), 90–105 (2000).
84. Q. Zhang et al., "Observed changes of temperature extremes during 1960–2005 in China: natural or human-induced variations?" *Theor. Appl. Climatol.* **106**(3), 417–431 (2011).

Biographies of the authors are not available.